Internal bremsstrahlung: Exact relativistic independent-particle-approximation calculations

T. Surić, R. Horvat, and K. Pisk

Ruđer Bošković Institute, P.O. Box 1016, Zagreb, Croatia

(Received 7 August 1992)

We have reformulated the relativistic theory of internal bremsstrahlung in electron capture (IBEC) and developed a numerical code for calculating a transition amplitude for any initial atomic state. All relativistic as well as screening effects are included within the independent-particle approximation. We have shown the advantage of the theory even in the pole-dominance region of the IBEC spectra, thus making it suitable for comparison with the observed spectra in experiments that search for light- and/or heavy-neutrino mass components. In addition, we have applied our code to study the interference effects in the IBEC transition amplitude of ^{163}Ho and found, in agreement with experimental data, a smaller interference suppression than predicted by several recent models.

I. INTRODUCTION

In 1981, De Rújula [1] was the first to put forward an idea that internal bremsstrahlung in electron capture (IBEC) could be used to investigate the possibility of nonzero electron-neutrino mass. He noted that the sensitivity for radiative p capture was considerably enhanced when the electron-capture (EC) Q value was sufficiently low to be in the x-ray region. The photon distribution is determined by a phase space that is mass dependent; the spectral end point is studied analogously as in β-decay experiments. Experimental investigations of the best candidates, ^{193}Pt and ^{163}Ho, set an upper limit of 500 eV [2] and 225 eV [3], respectively, to the mass of the electron neutrino.

In 1986, the CERN-ISOLDE group of Barge *et al.* [4] used the IBEC spectrum of ^{125}I to search for an admixture of heavy neutrinos, whereas the nonzero result for the corresponding antiparticle was reported earlier in the nuclear β-decay experiment by Simpson [5]. Simpson interpreted an anomaly in the β-decay spectrum of tritium as being due to the presence of a heavy neutrino of a mass of 17 keV, with an emission probability of a few percent. Subsequent beta-decay experiments, however, did not appear to confirm this effect [6]. For the same purpose, later on, Žlimen *et al.* [7] studied IBEC from ^{55}Fe and found no evidence for a heavy neutrino, in accordance with the finding of Barge *et al.*

Renewed interest in the heavy neutrino started in 1989 when Simpson and Hime [8] measured anew tritium and ^{35}S beta decays and again reported positive evidence for the 17-keV anomaly. More recently, the ^{35}S experiment was reported [9], while the Berkeley group of Sur *et al.* [10] measured the spectrum of ^{14}C; both experiments gave positive results. It is interesting that recent β-decay data have received some confirmation from the study of the IBEC in ^{55}Fe [11] and ^{71}Ge [12]. Both groups observed a kink or distortion in the IBEC spectra, indicating the emission of a heavy neutrino with a mass of 17 keV and 1% mixing with the electron neutrino.

Considering the large number of constraints which the 17-keV neutrino has to obey, one is forced to conclude that such a particle is unlikely to exist (see, e.g., Ref. [13]). Cosmology constrains such a neutrino to decay much faster than the age of the Universe or to have a sizable cross section for annihilation into practically massless particles. More importantly, considerations of double-beta-decay limits imply that the component of the electron-neutrino Majorana-type mass is less than a few eV's [14], and so one has to conclude that this particle is of Dirac type. However, recent detailed calculations based on supernova dynamics have yielded a limit on the mass of a Dirac neutrino of approximately 28 keV [15]. However, when the mixing is taken into account [16], it can be shown that a 17-keV neutrino with 1% mixing with the electron neutrino lies well inside the region excluded for Dirac neutrinos. Thus the supernova limit confronts the positive results of recent β-decay and IBEC experiments. However, a few models [17], where a 17-keV neutrino is a part of an almost degenerate pseudo-Dirac pair of states, can accommodate all these results.

Motivated by the 17-keV controversy, we have written a code for calculating the IBEC amplitude that is an extension of an earlier paper [18]. The code can be used to calculate the IBEC spectrum from any atomic state. Our calculations of IBEC spectra include all relativistic effects as well as exact screening within the independent-particle approximation (IPA) of the atom. We have performed calculations of IBEC spectra for ^{125}I and ^{193}Pt, as well as for ^{163}Ho and compared them with the spectra obtained in several versions of an extended Glauber-Martin theory.

II. PRESENT STATUS OF IBEC THEORY

The first calculations of IBEC spectra are due to Stueckelberg [19], Møller [20], and Morrison and Shiff [21], who developed a theory of IBEC spectra in allowed transitions, completely neglecting the Coulomb field of the nucleus. Glauber and Martin [22] and Martin and Glauber [23] performed calculations for IBEC, taking into account the atomic structure (nuclear Coulomb field,

but taking screening effects only approximately) and relativistic effects in radiative capture of 1s-state electrons. They predicted appreciable contributions from initial p-state electrons at lower photon energies; this was involved with the resonance structure of the $p \rightarrow s$ atomic transition.

Inteman [24] improved the calculations of Martin and Clauber [23] to obtain a simple method for calculating IBEC from 1s states. Zon [25] performed relativistic calculations for IBEC from L and M shells, whereas Zon and Rapoport [26] included transitions of an arbitrary order of forbiddance. A comprehensive review of older theoretical and experimental IBEC investigations can be found in the paper of Bambynek et al. [27].

De Rújula noted [1] that the IBEC spectrum can be exploited to search for the nonzero electron-neutrino mass. His main observation was that low-energy IBEC is predominantly p wave ($E1$ process) and that it interferes with $E1$ x-ray emissions following EC. He extended the nonrelativistic theory of Glauber and Martin below the x-ray region, because the interference turned out to be constructive when the end point of the IBEC spectrum lay below the energy of the characteristic x ray. Moreover, De Rújula made a further extension of the theory near poles in the sense that only a dominant pole term in the IBEC amplitude was evaluated directly, whereas the rest was approximated. This served to insert the experimental binding energies, widths, and intensities in a dominant-pole term to include the fine structure and also to make an explicit distinction between two time orders of the process ($Z \leftrightarrow Z - 1$ distinction). Further improvements [28] consisted in applying the sum-rule technique when calculating the effects of all poles from unfilled electron and continuum states, together with using more realistic atomic wave functions. Such models give a total IBEC spectrum that agrees with the absolute experimental data only to within a factor of 1.5–2 (see Fig. 3 in Ref. [28]). In addition, destructive interference can also occur [28,3] between the contribution to the IBEC amplitude from the dominant pole and contributions from all other pole terms and continuum states. The size and direction of interference effects depend on the photon energy, and in several atomic models, the case of ^{163}Ho reveals deep interference minima near the end points of $4p$ and $5p$ states. However, such a strong destructive interference is not confirmed by experimental data [3].

III. MODEL AND FORMALISM

The matrix elements for IBEC can be written in the usual theory [27] as

$$M_{fi} = \frac{ieG_F}{2\sqrt{2}\pi\omega} \delta(E_{max}^a - q - \omega)$$

$$\times \int d^3x \, d^3y \, \overline{\Phi}_f(\mathbf{x}) \Gamma_\mu \Phi_i(\mathbf{x}) \overline{\Psi}_\nu(\mathbf{x})$$

$$\times \Lambda^\mu S_\upsilon(\mathbf{x},\mathbf{y},\eta)\gamma \cdot \boldsymbol{\epsilon}^* e^{-i\mathbf{k}\cdot\mathbf{y}} \Psi_a(\mathbf{y}) . \quad (1)$$

Here we have employed the units $c = \hbar = 1$. The quantities Γ_μ and Λ_μ are defined as $\Gamma_\mu = \gamma_\mu(1 - \lambda_w \gamma_5)$, $\Lambda_\mu = \gamma_\mu(1 - \gamma_5)$, and the notation used is the same as in

Ref. [29]. The quantities Φ_i and Φ_f are the nuclear wave functions for the initial and final states, respectively. Ψ_ν and Ψ_a are the respective Dirac spinor wave functions for a neutrino and a bound electron. The photon is characterized by the momentum $\mathbf{k}$ and the polarization vector $\boldsymbol{\epsilon}$. E_{max}^a is the total energy available in the transition, and q and $\omega = |\mathbf{k}|$ are the energies of the neutrino and photon. $S_\upsilon(\mathbf{x},\mathbf{y},\eta)$ represents the Feynman propagator in the potential $V(r)$; $\eta = E_a - \omega$, and we consider that $|\eta| < m$. In addition, S_υ is a solution of the inhomogeneous Dirac equation

$$[\boldsymbol{\alpha}\cdot\mathbf{p} + \gamma^0 m + V(r) - \eta]S_\upsilon(\mathbf{x},\mathbf{y},\eta) = -\gamma^0 \delta^3(\mathbf{x}-\mathbf{y}) . \quad (2)$$

Our treatment of IBEC is based on an exact numerical evaluation of the matrix element (1) within the independent-particle approximation of the atom. It is fully relativistic. In the calculations we use the spherically symmetric relativistic self-consistent (RSC) Dirac-Slater potential $V(r)$ and the corresponding atomic wave functions obtained using the Liberman code [30]. For the nucleus we use a simple model of a uniformly charged shell of radius R.

Our treatment of IBEC is limited to allowed transitions [31] and does not make distinction between two time orders of the process ($Z \leftrightarrow Z - 1$ distinction). We discuss this point in more detail in Sec. IV. The treatment follows the procedure of Pisk, Pašagić, and Logan [18], which was originally developed for s-electron radiative capture, but can be applied to a capture from an arbitrary electron state. Following the procedure, instead of calculating the propagator $S_\upsilon(\mathbf{x},\mathbf{y},\eta)$ directly, we calculate the function

$$F(\mathbf{x},\eta) = \int d^3y \, S_\upsilon(\mathbf{x},\mathbf{y},\eta)\gamma\cdot\boldsymbol{\epsilon}^* e^{-i\mathbf{k}\cdot\mathbf{y}}\Psi_a(\mathbf{y}) . \quad (3)$$

In such a way, all intermediate states included in the propagator $S_\upsilon(\mathbf{x},\mathbf{y},\eta)$ are taken into account. The function $F(\mathbf{y},\eta)$ is a solution of the inhomogeneous Dirac equation

$$[\boldsymbol{\alpha}\cdot\mathbf{p} + \beta m + V(r) - \eta]F(\mathbf{x},\eta) = \gamma\cdot\boldsymbol{\epsilon}^* e^{-i\mathbf{k}\cdot\mathbf{x}}\Psi_a(\mathbf{x}) , \quad (4)$$

with the following boundary conditions:

$$\int F^\dagger(\mathbf{x},\eta)F(\mathbf{x},\eta)d^3x < \infty, \quad |\eta| < m , \quad (5a)$$

$$\lim_{r \to \infty} F(\mathbf{x},\eta) = 0 , \quad r = |\mathbf{x}| . \quad (5b)$$

In terms of $F(\mathbf{y},\eta)$ and after the nuclear weak current has been averaged over the nuclear volume, the matrix element M_{fi} can be written as

$$M_{fi} = \frac{ieG_F}{2\sqrt{2}\pi\omega} \delta(E_{max}^a - q - \omega)B_\mu$$

$$\times \int_{\Delta V} d^3x \, \overline{\Psi}_\nu(\mathbf{x})\Lambda^\mu F(\mathbf{x},\eta)\Psi_a(\mathbf{x}) . \quad (6)$$

The spherical symmetry of the potential allows us to use the partial-wave expansion of the functions $F(\mathbf{x},\eta)$ and Ψ_ν, the multipole expansions of the photon field, and to perform the angular integration in Eq. (6) analytically. In the partial-wave expansion of the function $F(\mathbf{x},\eta)$, the

radial component of the partial wave is denoted by $F_{L,\lambda}^{\kappa_1}(r,\eta)$. $F_{L,\lambda}^{\kappa_1}(r,\eta)$ is a solution of an inhomogeneous Dirac equation with an inhomogeneous term (driving term) that is a product of the radial component of the photon multipole (described by quantum numbers L,λ) and the radial components of the bound-electron wave function Ψ_a. Near the origin, the solution of this equation satisfies the boundary condition of Eq. (5a) and should be of the form

$$F_{L,\lambda}^{\kappa_1}(r,\eta)=r^{\beta+1}\sum_j F_j r^i+\alpha_{L,\lambda}^{\kappa_1} r^{\gamma_1}\sum_j Y_j r^j , \qquad (7)$$

where $\gamma_1=|\kappa_1|$ and $\beta=\gamma+L-\lambda$, $\gamma=|\kappa|$. The first term in Eq. (7) is a particular solution of the inhomogeneous radial equation near the origin. The second term in (7) is a solution of the inhomogeneous radial equation near the origin, which is regular for $r=0$. Since the potential is nonsingular at the origin, we have chosen $Y_0=\binom{0}{1}$ for $\kappa_1>0$ and $Y_0=\binom{1}{0}$ for $\kappa_1<0$.

At infinity, the solution should behave as [see Eq. (5b)]

$$F_{L,\lambda}^{\kappa_1}(r,\eta) \underset{r\to\infty}{\longrightarrow} Fe^{-\lambda r}, \quad \lambda=(m^2-\eta^2)^{1/2} . \qquad (8)$$

The solution can be found numerically. We apply the method of Brown, Peierls, and Woodward [32], integrating the inhomogeneous and homogeneous differential equations outward from the origin and inward from a distant point where it can be assumed that the inhomogeneous term vanishes. The constant α^{κ_1} is fixed, demanding that these two solutions (inward and outward) should be equal. This can be performed at an intermediate point.

Finally, radial integration has to be performed in (6). Since our calculation of IBEC is limited to allowed transitions, it is appropriate, when performing radial integration, to keep only the lowest-order term in a series expansion of the functions $F(x,\eta)$ and Ψ_ν over the nuclear radius R.

After performing radial integration, we square the amplitude and perform appropriate momentum and spin summations. In such a way, the IBEC differential cross section $dW^a/d\omega$ can be obtained as

$$\frac{dW_{IB}^a}{d\omega}=\frac{2\alpha G_F^2|B|^2}{\pi}\omega(Q-\omega-|B_a|)$$
$$\times[(Q-\omega-|B_a|)^2-m_\nu^2]^{1/2}$$
$$\times\sum\frac{1}{L(L+1)}\frac{1}{2}[1+(-1)^{l_1+l+L+\lambda+1}]\alpha_{L,\lambda}^{\kappa_1} , \qquad (9)$$

where α^{κ_1} is a constant from Eq. (7). The summation in Eq. (9) includes $\kappa_1=-1,1$ (allowed transitions) and all L that, together with j_1 (total angular momentum of the electron in the propagator) and j (total angular momentum of the bound electron), satisfy the triangle rule.

The total probability for the nonradiative capture of an electron from the state a within the same model is

$$W_{EC}^a=\frac{2G_F^2|B|^2}{9\pi}\omega(Q-|B_a|)[(Q-|B_a|)^2-m_\nu^2]^{1/2}A_\kappa^2 . \qquad (10)$$

Here A_κ is the coefficient of the leading term in the series expansion of the bound-electron wave function around the origin. Bound-electron wave functions are normalized to unity.

More details on the formalism as well as on the methods of solving differential equations can be found in Ref. [18]. The only difference is that in the present paper we employ a finite nucleus instead of a point nucleus. This implies the nonsingular behavior of electron wave functions near the origin. More details on the methods and techniques employed can also be found in Refs. [32,33] where other atomic processes (Rayleigh scattering, Compton scattering) were treated within the same model and using similar methods.

Our computer code calculates the IBEC spectrum normalized to EC. It uses as input the numerically given atomic IPA potential and electron wave functions. We have used the Coulomb potential and the relativistic hydrogen model of the atom when making comparisons with various versions of the Glauber-Martin theory, but otherwise we have employed the relativistic self-consistent potential and electron wave functions obtained using the Liberman code.

IV. RESULTS AND DISCUSSION

In this section we present the results of the calculation of IBEC spectra obtained using our code (exact IPA calculation) and compare them with the results of various versions of the Martin-Glauber theory and with experiments.

The Martin-Glauber theory [22,23] takes into account relativistic effects and the Coulomb field of the nucleus. However, they limited their fully relativistic calculations to 1s-state capture only. For higher states, their calculation is nonrelativistic and the effect of the Coulomb field is taken only to the lowest order in $Z\alpha$. Screening effects are taken into account approximately, multiplying the unscreened results for the IBEC amplitude by the ratio of screened to unscreened initial-state wave functions, evaluated in the neighborhood of the origin. In this way, only the modification of the initial electron wave function, caused by scattering, is taken into account. The second effect of screening, the alteration in the structure of the electron propagator, is expected to be small. It is argued by Martin and Glauber [23] that this procedure to take screening into account should be reasonable for photon energies above the characteristic x-ray region. The accuracy of this simple approximation scheme was quantitatively established on the example of the 2p state of Fe. Screening effects in nonrelativistic IBEC were discussed by Iwinski, Kim, and Pratt [34].

De Rújula [1] extended the theory of Glauber and Martin to the pole region in the sense that only a dominant-pole term in the IBEC amplitude is evaluated exactly, whereas the rest is approximated. This serves to

insert the experimental binding energies and widths so that the poles appear in their right place and with the right intensity. This approach is correct only near the poles.

In Figs. 1–6 the results of our exact IPA calculations for ^{125}I are compared with the results of the Martin-Glauber theory calculated from the paper by Inteman [24] and with the results of De Rújula [1]. Calculations were performed using the RSC and Coulomb potentials (to demonstrate the accuracy of simple Glauber-Martin scheme for inclusion of screening). Calculations with the Coulomb potential were performed using self-consistent binding energies in the kinematic factor in (9) and (10). All these spectra were normalized to the total EC.

The spectrum of the radiative ^{125}I 1s-electron capture, normalized to the 1s nonradiative capture, is shown in Fig. 1. The results of the exact IPA calculation performed using the RSC potential are denoted by crosses and those obtained using the Coulomb potential by circles. The results of the relativistic Martin-Glauber theory, calculated from the paper by Inteman [24], are also shown (solid lines). Good agreement between the results obtained using the Coulomb potential (exact IPA Coulomb calculation and Martin-Glauber calculation) and the self-consistent potential shows that the alteration in the structure of the propagator, caused by screening, is negligible. The modification of the wave function of the initial electron cancels out because of the normalization to nonradiative capture, which is dominated by the capture from the 1s state.

For higher shells, relativistic calculations were performed by Zon [25] (for L and M shells) and by Pisk, Pošagić, and Logan [18] (2s subshell). Zon reported the construction of a computer program that permits numerical evaluation of the amplitude for the radiative capture from L and M shells with all Coulomb and relativistic effects included. The spectra of ^{165}Er were analyzed. The results obtained were compared with Glauber-Martin nonrelativistic calculations where only terms through first order in $Z\alpha$ were retained.
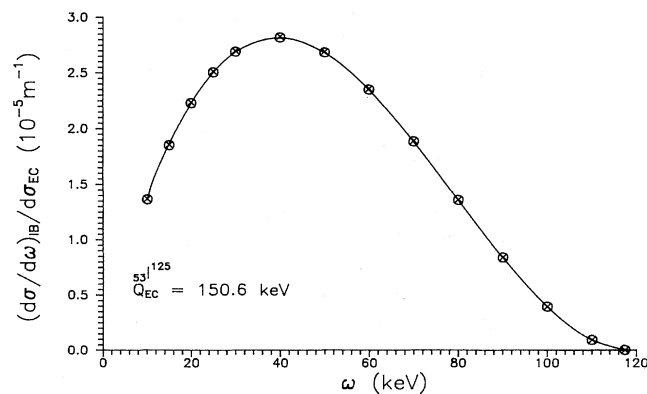
For the 2s-state capture, the results obtained by Zon

show a sharp resonance that is associated with a forbidden 2s-1s atomic transition and therefore modifies the result of Glauber and Martin only in the binding-energy region. Elsewhere, the results of Zon and Glauber and Martin are indistinguishable. Contrary to the results of Zon, Pisk, Pašagić, and Logan [18] calculated a modification of the results of Glauber and Martin not only in the resonance region, but also for higher photon energies where their values are always smaller. It should also be noted that the shape of their 2s radiative-capture spectrum near the resonance is different from that of Zon; namely, the spectrum of Pisk, Pašagić, and Logan exhibits a pronounced minima for energies slightly above the resonance.

We have performed calculations for L and M states of ^{125}I using both the Coulomb and RSC potentials. For the 2s state, the shape of the spectrum and the values are very similar to those obtained by Pisk, Pašagić, and Logan. To demonstrate the accuracy of the simple Glauber-Martin scheme (to include the screening), we have applied this scheme to our results obtained using the Coulomb potential. In calculations with the Coulomb potential, binding energies obtained with the RSC potential have been used to keep the same kinematical conditions. The results of the calculation of the 2s and 3s IBEC spectra (normalized to the total EC) are compared with the nonrelativistic Glauber-Martin theory calculated from the paper of Intemann, as shown in Figs. 2 and 3. These results show that Coulomb and relativistic effects significantly modify the results of the Glauber-Martin theory for higher s states not only in the resonant region, but also at higher energies. In the low-energy region (below the indicated pole), the 2s IBEC exact IPA results and Glauber-Martin results approach each other. For 3s IBEC, such agreement in this energy region is not to be expected since other resonances occur there. It is also evident that the Glauber-Martin scheme to include the screening is very accurate in the whole energy region except near the resonances.
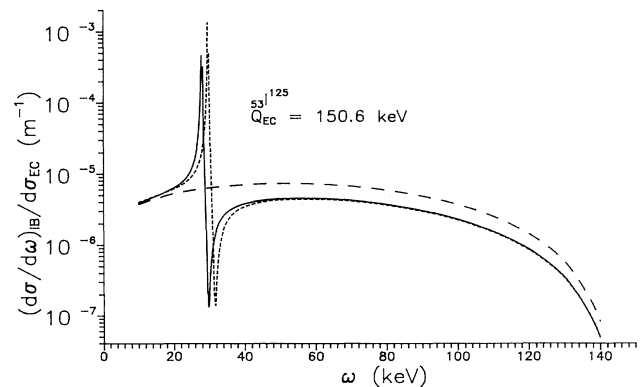

FIG. 1. K-shell IBEC spectra for ^{125}I. Comparison between the relativistic Glauber-Martin theory calculated from Ref. [24] (solid line), exact IPA calculation with the RSC potential ($\times$), and exact IPA calculation with the Coulomb potential ($\bigcirc$).

FIG. 2. IBEC spectra for radiative capture from the 2s state of ^{125}I. Comparison between the nonrelativistic Martin-Glauber theory calculated from Ref. [24] (long-dashed line), exact IPA calculation with the RSC potential (solid line), and exact IPA calculation with the Coulomb potential (short-dashed line) after multiplication by the screening factor.
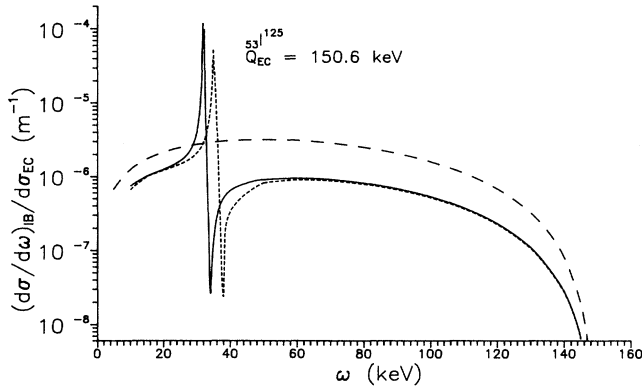
FIG. 3. IBEC spectra for radiative capture from the $3s$ state of ^{125}I. Comparison between the nonrelativistic Martin-Glauber theory calculated from Ref. [24] (long-dashed line), exact IPA calculation with the RSC potential (solid line), and exact IPA calculation with the Coulomb potential after multiplication by the screening factor (short-dashed line).

The results of the calculation of the radiative capture from the $2p$ and $3p$ states of ^{125}I (normalized to the total EC) are shown in Figs. 4–7. The contributions from $p_{1/2}$ and $p_{3/2}$ states are added up. Exact IPA results are compared with the nonrelativistic calculations of De Rújula and Glauber and Martin. As already stated, the results of De Rújula give correct values in the pole region. As can be seen from Figs. 4 and 5, the results of our calculation using the RSC potential and the results of De Rújula's simple formula agree very well near the pole. Although the resonant widths in our model are zero, this does not alter the results in the region of interest. In this region (which is usually, at least, a few hundred eV far from the pole), the real part of the propagator denominator is much larger than the imaginary one. The position
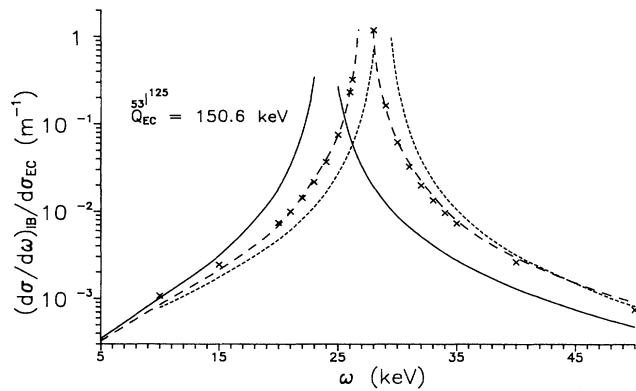

FIG. 4. IBEC spectra for radiative capture from the $2p$ state of ^{125}I. Comparison between the nonrelativistic Martin-Glauber theory calculated from Ref. [24] (solid line), extended Glauber-Martin theory of De Rújula [pole approximation given by Eqs. (10.5a) and (10.5b) in Ref. [1]] (long-dashed line), exact IPA calculation with the RSC $(Z-1)$ potential ($\times$), and exact IPA calculation with the Coulomb $(Z-1)$ potential after multiplication by the screening factor (short-dashed line). Contributions from $2p_{1/2}$ and $2p_{3/2}$ are added up.
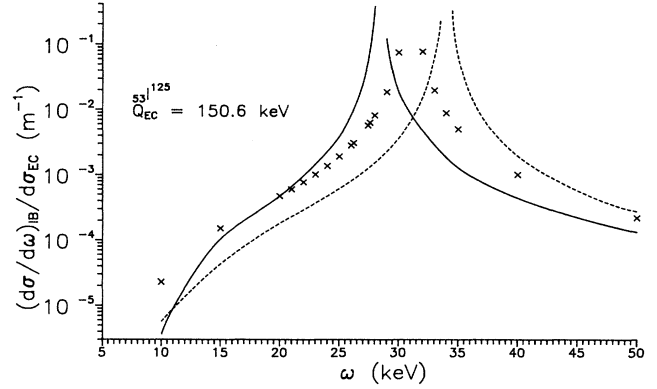

FIG. 5. IBEC spectra for radiative capture from the $3p$ state of ^{125}I. Comparison between the nonrelativistic Martin-Glauber theory calculated from Ref. [24] (solid line), exact IPA calculation with the RSC $(Z-1)$ potential ($\times$), and exact IPA calculation with the Coulomb $(Z-1)$ potential after multiplication by the screening factor (dashed line). Contributions from $3p_{1/2}$ and $3p_{3/2}$ are added up.

of the poles is determined by RSC eigenvalues which are in fair agreement with experimental binding energies. Other calculations (exact IPA calculation with the Coulomb potential and the Glauber-Martin calculation) incorrectly reproduce the position of the resonances also owing to the use of the unscreened and/or nonrelativistic propagator.

For higher energies, the results of De Rújula deviate from exact IPA calculations with the RSC potential. In this region, the Martin-Glauber theory is more appropriate, as can be seen from Figs. 6 and 7. Very good agreement is obtained between the exact IPA calculation using the RSC potential and the results using the Coulomb potential where the Glauber-Martin scheme to include screening is applied.

The case of ^{193}Pt, which has a Q_{EC} value that falls 20 keV below the $2p \rightarrow 1s$ resonance point, is very suitable for a test of the theory for higher shells. Although the capture is first-forbidden nonunique, the spectrum has the shape of allowed transitions since $Q_{EC}R \ll Z\alpha$ [27].
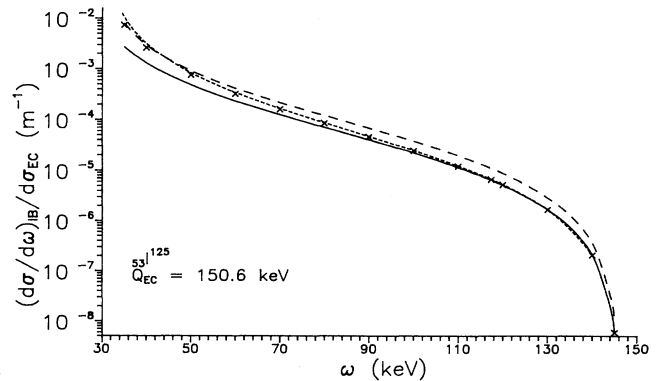

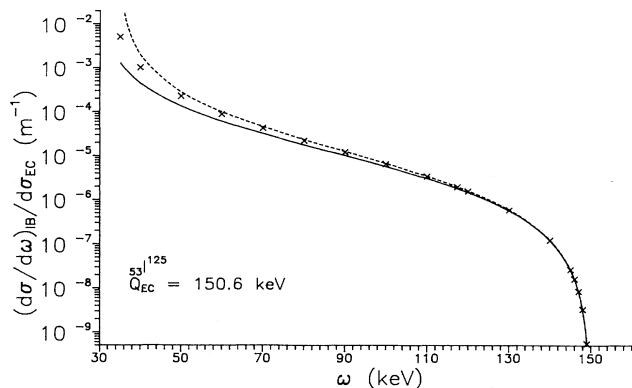FIG. 6. Same as Fig. 4, but with the high-energy region of the spectrum.

FIG. 7. Same as Fig. 5, but with the high-energy region of the spectrum.

FIG. 9. IBEC spectra for radiative capture from the $2p$ state of ^{193}Pt, otherwise as in Fig. 8. This figure corresponds to Fig. 4 of Ref. [28].

In the paper of Riisager et al. [28], IBEC spectra were calculated in two versions of the extended Glauber-Martin theory. The extension consisted in applying the sum-rule technique to calculate the effects of all poles from unfilled electron and continuum states, together with the using of the more realistic atomic wave functions. The results of the calculation were compared with experimental data. The comparison showed that all main features of the spectra were in agreement with the results of the calculation, although the absolute intensities agreed only within a factor or 1.5–2. It was found that the simple hydrogenic model hit right on the experimental points, and in their opinion this performance of the simple model seemed to be fortuitous.

Partly motivated by this discrepancy, we have used our code to calculate the IBEC spectrum for ^{193}Pt. The results of exact IPA calculations are shown in Figs. 8–10. The model used in this paper does not make an explicit distinction between two time orders of the process. To estimate the uncertainty caused by that, we have per-
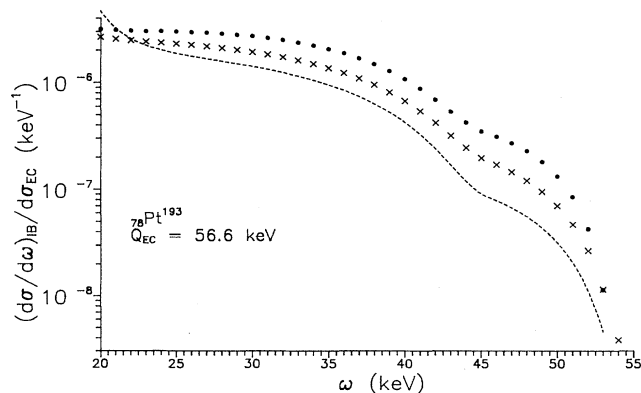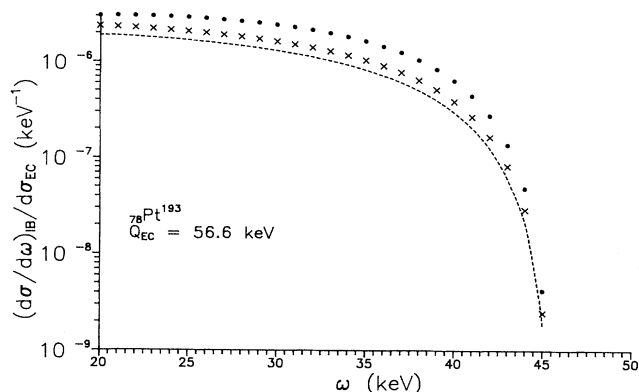
formed the calculations in both the ^{193}Ir $(Z-1)$ and ^{193}Pt (Z) RSC potentials and found that the difference is negligible. In all figures where the process is dominated by pole terms, we show only the results performed in the $Z-1$ potential. (This corresponds to the time order of the process where the electron capture precedes the radiative transition.) Figures 8–10 also show the results of exact IPA calculations with the unscreened Coulomb $(Z-1)$ potential multiplied by a screening factor, and the results of the simple hydrogenic model [1] (which hit right on the experimental points of Ref. [28]) are also shown.

As can be seen from Figs. 8–10, although the model used consistently takes into account all screening and relativistic effects on the single-particle-approximation level, it cannot explain the factor of 1.5–2 discrepancy between theory and experiment. Namely, exact IPA results obtained with the RSC potential are approximately the same as those obtained using model II from Ref. [28] and are consistently smaller by this factor than the experi-
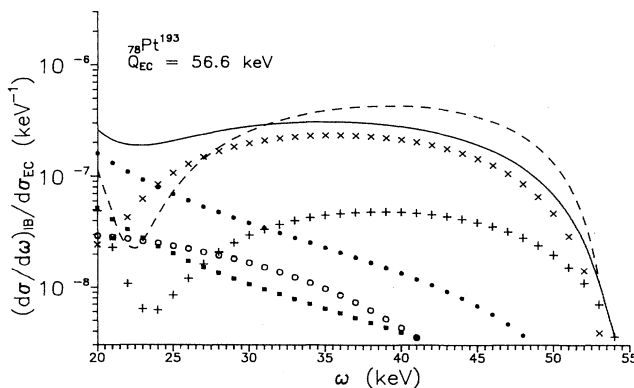

FIG. 8. Total IBEC spectrum of ^{193}Pt. Comparison between exact IPA calculation with the RSC potential ($\times$), exact IPA calculation with the Coulomb potential after multiplication by the screening factor (dashed line), and the simple hydrogenic model of Ref. [1] ($\bullet$). This figure corresponds to Fig. 3 of Ref. [28].

FIG. 10. IBEC spectra from higher states of ^{193}Pt obtained in exact IPA with the RSC $(Z-1)$ potential: $3p$ IBEC spectra ($\times$), $4p$ spectra ($+$), $2s+3s+4s$ spectra ($\circ$), $3d$ spectra ($\bullet$), and $4d$ spectra ($\blacksquare$). The solid line represents the total contribution from these states. The results of De Rújula's pole approximation used for the calculation of $3p+4p$ spectrum are indicated by dashed line.

mental values. The results obtained using the Coulomb unscreened potential are even smaller, which is consistent with the behavior of the spectrum below the p poles, as seen from Figs. 4 and 5.

Of all the isotopes which decay by electron capture, ^{163}Ho is perhaps the best suited for use in a light-neutrino mass experiment. ^{163}Ho has the lowest Q_{EC} ($\simeq 2.8$ keV) value known; the neutrino is emitted with low energy, and a neutrino mass of a few tens eV might have a pronounced effect on the decay properties. K and L captures are energetically forbidden, and therefore capture occurs from M and higher shells. In the case of radiative electron capture, only N and higher shells contribute to the experimentally interesting region—the high-energy end of the photon spectrum. It is to be expected that the shape of the spectrum in this region might be rather sensitive to the model used. Uncertainties in the shape of the spectrum can make the interpretation of experimental data difficult.

In their work, Riisager et al. [28] calculated the IBEC spectrum of ^{163}Ho using the same model as for ^{193}Pt and predicted the occurrence of an interference minimum near the end point, which reduced the expected intensity and also complicated the shape of the spectrum. Springer, Bennett, and Baisden [3] measured the IBEC spectrum of ^{163}Ho, compared the data with the IBEC model similar to that of Riisager et al., and found that interference suppressions were smaller than predicted. In their opinion, this discrepancy indicated that the atomic models used in their calculations were inadequate. They reported an upper limit of 225 eV for the mass of the electron neutrino and concluded that improvements of this result were severely limited by uncertainties in atomic interference effects.

Using the code, we have performed calculations of the IBEC spectrum for ^{163}Ho with the RSC potential for ^{163}Dy. The results are shown in Figs. 11–14 for the region of the spectrum above 1.8 keV, which is the most sensitive region to the neutrino mass.
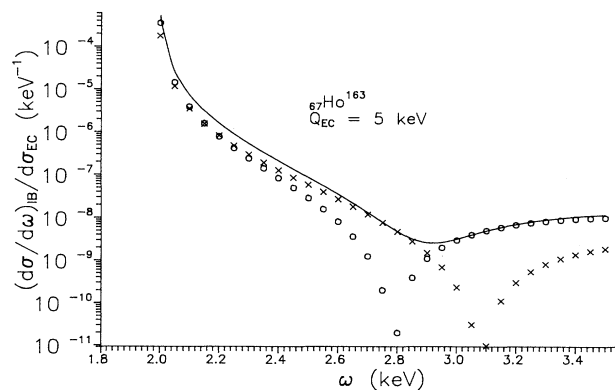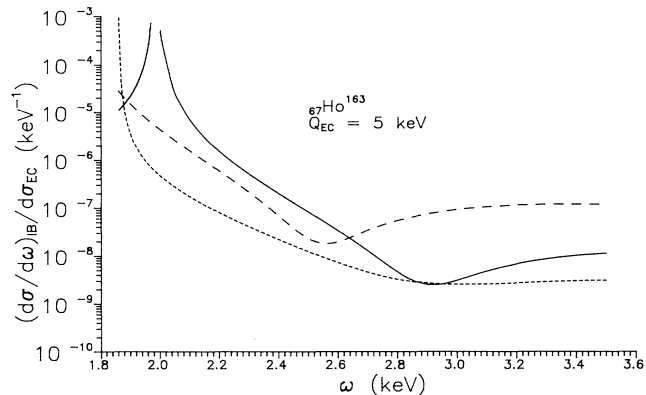
In Fig. 11 we present the results of these calculations

FIG. 12. IBEC spectra of ^{163}Ho from the states with the most dominant contributions obtained in the exact IPA with the RSC $(Z-1)$ potential: $4p$ IBEC spectra (long-dashed line), $5p$ spectra (solid line), and $4d$ spectra (short-dashed line). $Q_{EC}=5$ keV is assumed.

for the capture from $5p$ states. Contributions from $5p_{1/2}$ and $5p_{3/2}$ are shown separately. Here we used the value $Q_{EC}=5$ keV, as in Ref. [28], to shift the end point of the spectrum out of the region of interference minima. It should be noted that, while the energy difference between $5p_{1/2}$ and $5p_{3/2}$ eigenvalues is only a few eV, the minima of the $5p_{1/2}$ and $5p_{3/2}$ spectra are shifted by approximately 300 eV. The combined contribution shows less pronounced suppression than those obtained by Riisager et al. The IBEC spectra from other subshells show similar behavior, and those with largest contributions are presented in Fig. 12. Again, the value $Q_{EC}=5$ keV was used. Contributions from the same subshells with the value $Q_{EC}=2.82$ keV are shown in Fig. 13, and the total IBEC spectrum is presented in Fig. 14. All Ho spectra are normalized to total EC.

Comparing exact IPA results obtained using the RSC potential with those of Riisager et al., we have found that our calculation gives a much simpler structure of the total IBEC spectrum, although interference minima are
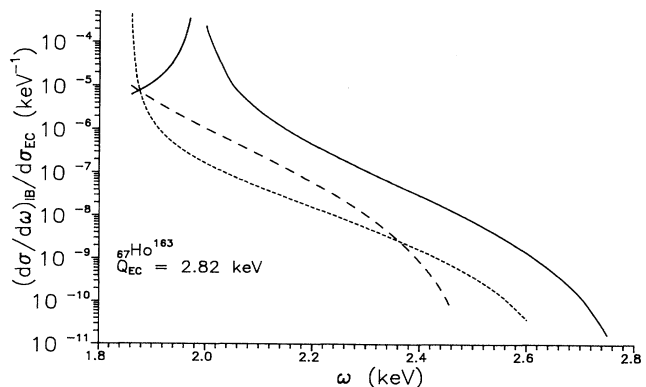
FIG. 11. $5p$ radiative capture of ^{163}Ho obtained in the exact IPA model with the RSC $(Z-1)$ potential (solid line). $Q_{EC}=5$ keV is assumed. Contributions from the states $5p_{1/2}$ ($\times$) and $5p_{3/2}$ ($\bigcirc$) are shown separately. Interference minima are shifted much more than expected from the corresponding eigenvalue shift.

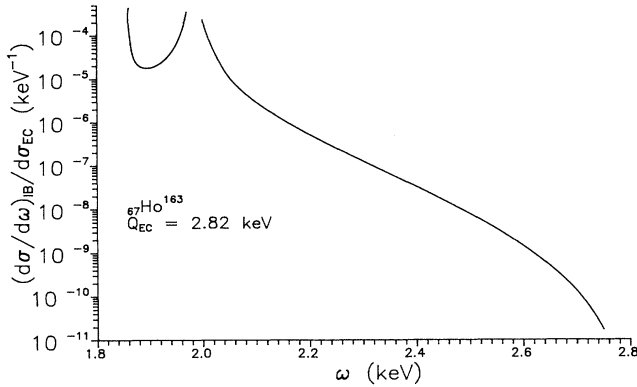FIG. 13. Same as Fig. 12, except that $Q_{EC}=2.82$ keV is used.

FIG 14. Total IBEC spectrum of ^{193}Ho calculated in the exact IPA model using the RSC potential.

present near the end of the spectrum. In addition, the intensity of the spectrum is higher near the kinematical end, which might be promising in neutrino mass experiments. We believe that our results might explain the discrepancy found in the experiment performed by Springer, Bennett, and Baisden [3].

V. CONCLUSIONS

Calculations of the IBEC spectra presented here have been compared with the spectra obtained in the Martin-Glauber theory as well as in several extended versions. Although our results for $1s$ IBEC are in excellent agreement with previous calculations, higher s IBEC spectra show disagreement with Zon's results, not only near the resonance, but also for higher photon energies, including the interference dip slightly above the resonance. Binding energies, obtained using the RSC-potential method, differ from the experimental ones by at most a few percent, and so the code works fairly well near the isolated pole. In addition, the contribution from all other poles, contrary to De Rújula's extended versions, has been calculated consistently. The code calculations confirm the validity of the inclusion of the screening in the manner of Martin and Glauber, showing disagreement only in the vicinity of x-ray resonances. Comparing our results with experimental data for ^{193}Pt, we can see that the disagreement in absolute intensities is similar to that obtained with model II of Riisager et al. The code has been applied to ^{163}Ho, which owing to its low Q value, is a candidate for neutrino mass measurements via IBEC. Primarily, because of fine-structure effects, our results show much smaller destructive interference minima near the end point, hence making the slope less complicated than stated before.

[1] A. De Rújula, Nucl. Phys. B188, 414 (1981).
[2] B. Jonson, J. U. Andersen, G. J. Beyer, G. Charpak, A. De Rújula, B. Elbek, H. Å. Gustafsson, P. G. Hansen, P. Knudsen, E. Lægsgaard, J. Pedersen, and H. L. Ravn, Nucl. Phys. A396, 479c (1983).
[3] P. T. Springer, C. L. Bennett, and P. A. Baisden, Phys. Rev. A 35, 679 (1987).
[4] M. J. G. Borge, A. De Rújula, P. G. Hansen, B. Jonson, G. Nyman, H. L. Ravn, K. Riisager, and the ISOLDE Collaboration, Phys. Scr. 34, 591 (1986).
[5] J. J. Simpson, Phys. Rev. Lett. 54, 1891 (1985).
[6] T. Altzitzoglou et al., Phys. Rev. Lett. 55, 799 (1985); T. Ohi et al., Phys. Lett. 160B, 322 (1985); V. M. Datar et al., Nature 318, 547 (1985); J. Markey and F. Boehm, Phys. Rev. C 32, 2215 (1985); A. Apolikov et al., Pis'ma Zh. Eksp. Teor. Fiz. 42, 233 (1985) [JETP Lett. 42, 289 (1985)]; D. W. Hetherington et al., Phys. Rev. C 36, 1504 (1987).
[7] I. Žlimen, A. Ljubičić, S. Kaučić, and B. A. Logan, Phys. Scr. 38, 539 (1988).
[8] J. J. Simpson and A. Hime, Phys. Rev. D 39, 1825 (1989); A. Hime and J. J. Simpson, ibid. 39, 1837 (1989).
[9] A. Hime and N. A. Jelley, Phys. Lett. 257, 441 (1991).
[10] B. Sur et al., Phys. Rev. Lett. 66, 2444 (1991).
[11] E. B. Norman et al., in Proceedings of the 14th Europhysics Conference on Nuclear Physics, Bratislava, Czechoslovakia, 1990 (unpublished).
[12] I. Žlimen, A. Ljubičić, S. Kaučić, and B. A. Logan, Phys. Rev. Lett. 67, 560 (1991).
[13] G. Gelmini, S. Nussinov, and R. D. Peccei, Int. J. Mod. Phys. A 7, 3141 (1992).
[14] Particle Data Group, Phys. Lett. B 239, 1 (1990).
[15] R. Gandhi and A. Burrows, Phys. Lett. B 246, 149 (1990);

261, 519(E) (1990).
[16] M. Turner, Phys. Rev. D 45, 1066 (1991); J. Pantaleone, Fermilab Report No. 91/18-T, 1992.
[17] R. Barbieri and L. Hall, Nucl. Phys. B364, 27 (1991); E. Ma, Phys. Rev. Lett. 68, 1981 (1992).
[18] K. Pisk, V. Pašagić, and B. A. Logan, Phys. Rev. C 21, 1525 (1980).
[19] E. C. G. Stueckelberg, Nature 137, 1070 (1936); Helv. Phys. Acta 9, 533 (1936).
[20] C. Møller, Pys. Z. Sowjetunion 11, 9 (1937).
[21] P. Morrison and L. I. Schiff, Phys. Rev. 58, 24 (1940).
[22] R. J. Glauber and P. C. Martin, Phys. Rev. 104, 158 (1956).
[23] P. C. Martin and R. J. Glauber, Phys. Rev. 109, 1307 (1958).
[24] R. L. Intemann, Phys. Rev. C 3, 1 (1971).
[25] B. A. Zon, Yad. Fiz. 13, 963 (1971) [Sov. J. Nucl. Phys. 13, 554 (1971)].
[26] B. A. Zon and L. P. Rapoport, Yad. Fiz. 7, 528 (1968) [Sov. J. Nucl. Phys. 7, 330 (1968)].
[27] W. Bambynek, H. Behrens, M. H. Chen, B. Crasemann, M. L. Fitzpatrick, K. W. D. Ledingham, H. Genz, M. Mutterer, and R. L. Intemann, Rev. Mod. Phys. 49, 77 (1977).
[28] K. Riisager, A. De Rújula, P. G. Hansen, B. Jonson, and H. L. Ravn, Phys. Scr. 31, 321 (1985).
[29] J. D. Bjorken and S. D. Drell, Relativistic Quantum Mechanics (McGraw-Hill, New York, 1964).
[30] D. Liberman, D. T. Cromer, and J. Walker, Comput. Phys. Commun. 2, 107 (1971).
[31] The same tretament can be applied in the case of the first-forbidden nonunique transition if $Q_{EC}R \ll Z\alpha$ (see Ref.

[27]).

[32] G. E. Brown, R. E. Peierls, and J. B. Woodward, Proc. R. Soc. London A **227**, 51 (1954).

[33] L. Kissel, R. H. Pratt, and S. C. Roy, Phys. Rev. A **22**,

1970 (1980); T. Suric, P. M. Bergstrom, K. Pisk, and R. H. Pratt, Phys. Rev. Lett. **67**, 189 (1991).

[34] Z. R. Iwinski, Y. S. Kim, and R. H. Pratt, Phys. Rev. C **19**, 1924 (1979).